

## ELECTROMAGNETIC PROPAGATION AND ABSORBING PROPERTY OF FERRITE-POLYMER NANOCOMPOSITE STRUCTURE

H. Bayrakdar\*

Department of Electric and Electronic Engineering, Hakkari University, Hakkari, Turkey

**Abstract**—We have synthesized ferrite-polymer nanocomposite structures and theoretically and experimentally investigated electromagnetic propagation, absorption properties of these nanocomposite materials at 8–20 GHz in microwave guides. The microwave properties of the samples were investigated by transmission line method, and reflection loss of  $-59.60$  dB was found at 12 GHz for an absorber thickness of 2 mm. These nanocomposites may be attractive candidates for microwave absorption materials.

### 1. INTRODUCTION

In recent years, the applications of electromagnetic (EM) wave have been very useful in high GHz ranges, including wireless telecommunication systems, radar, local area network, medical equipment, etc. [1–4]. With applications of electromagnetic (EM) wave in the high GHz ranges, the electromagnetic interference (EMI) problems have attracted more attention recently due to the extensive growth in the application of electronic devices and security, such as computer local area networks, mobiles phones, laptops, microwave oven, etc. [5–7].

Ferrites serve as better electromagnetic interference (EMI) suppressors than their dielectric counterparts on account of their excellent magnetic properties. Ferrite materials exhibit various electrical and magnetic properties of which complex permeability and complex permittivity, in particular, are important in determining their high frequency characteristics [8–11].

---

*Received 23 July 2012, Accepted 20 August 2012, Scheduled 5 September 2012*

\* Corresponding author: Harun Bayrakdar (habay78@yahoo.com).

In this work, we synthesized ferrite-polymer nanocomposite structures, and theoretically and experimentally investigated electromagnetic propagation, absorption properties of nanocomposite materials thin films at 8–20 GHz in microwave guides. The microwave properties of samples were investigated using network analyzer, and measurements were made by vibration sample magnetometer (VSM) technique.

## 2. THEORY

The two methods generally are used for materials characterization with network analyzer. They are:

1. Free Space Method
2. Transmission Line Method

### 2.1. Free Space Method

Free space is an important wave transmission scheme in communication and materials research. In radar and satellite communication, electromagnetic waves propagate through free space. In materials property characterization, free space provides much flexibility in studying electromagnetic materials under different conditions [12].

In recent years, there has been increasing interest in using free space techniques for the measurement of electromagnetic properties of materials. Because horn lens antennas have far field focusing ability, it is possible to make accurate free space measurements at microwave frequencies [12].

But this method may not be good for small samples. So we used transmission line method which can be used for this purpose [13].

### 2.2. Transmission Line Method

In a transmission/reflection method, the material under test is inserted in a piece of transmission line, and the properties of the material are deduced on the basis of the reflection from the material and the transmission through the material [13]. This method is widely used in the measurement of electromagnetic properties of materials. Because microwave guides have field focusing ability, it is possible to make accurate measurements at microwave frequencies [13]. Electromagnetic waves propagate through microwave guides. The samples are put in two waveguides, and experimental investigation is carried out.

Figure 1(a) shows a rectangular waveguide with width  $a$  and height  $b$ . Rectangular waveguides can transmit TE and TM modes. Usually, two subscripts  $m$  and  $n$  are used to specify TE or TM modes,

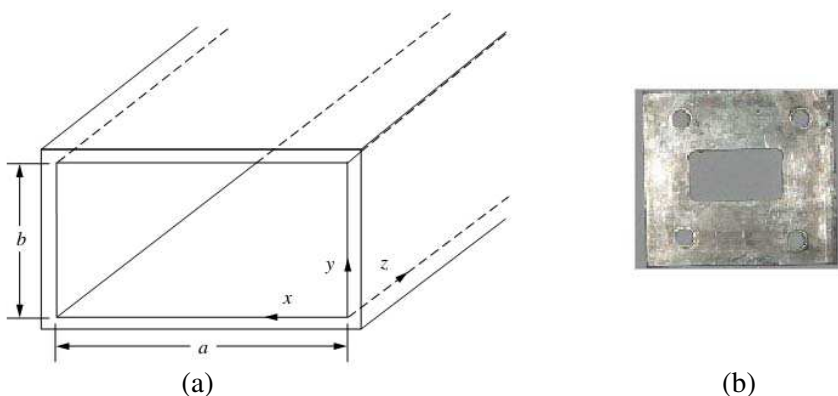


**Figure 1.** (a) Rectangular waveguide. (b) Special manufacture sample holder.

so the propagation mode is often denoted as  $TE_{mn}$  or  $TM_{mn}$ . The subscript “ $m$ ” indicates the number of changing cycles along width  $a$ , while the subscript “ $n$ ” indicates the number of changing cycles along height  $b$  [12].

The field components of  $TE_{mn}$  wave are

$$\begin{aligned}
 H_x &= A \frac{\gamma_{mn}}{k_c^2} \frac{m\pi}{a} \sin\left(\frac{m\pi}{a}x\right) \cos\left(\frac{n\pi}{b}y\right) \\
 H_y &= A \frac{\gamma_{mn}}{k_c^2} \frac{n\pi}{a} \cos\left(\frac{m\pi}{a}x\right) \cos\left(\frac{n\pi}{b}y\right) \\
 H_z &= A \cos\left(\frac{m\pi}{a}x\right) \cos\left(\frac{n\pi}{b}y\right) \\
 E_x &= Z_{TE} H_y \\
 E_y &= -Z_{TE} H_x \\
 E_z &= 0
 \end{aligned} \tag{1}$$

The constant  $A$  is related to the power of the wave. The parameters  $\gamma_{mn}$  and  $k_c$  are listed in Table 1 [12].

**Table 1.** Properties of empty rectangular waveguide.

	$TE_{mn}$ Mode	$TM_{mn}$ Mode
Cutoff wave number, $k_c$	$\sqrt{\left(\frac{m\pi}{a}\right)^2 + \left(\frac{n\pi}{b}\right)^2}$	$\sqrt{\left(\frac{m\pi}{a}\right)^2 + \left(\frac{n\pi}{b}\right)^2}$
Propagation constant	$\sqrt{k_c^2 + k_0^2}$	$\sqrt{k_c^2 + k_0^2}$

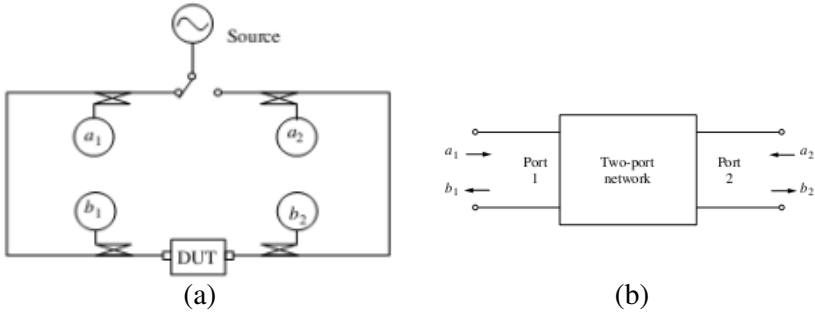


**Figure 2.** (a) The block diagram for network analyzer. (b) A two port network with “ $a$ ”s and “ $b$ ”s defined.

The field components of  $TM_{mn}$  wave are:

$$\begin{aligned}
 E_x &= B \frac{\gamma_{mn}}{k_c^2} \frac{m\pi}{a} \cos\left(\frac{m\pi}{a}x\right) \sin\left(\frac{n\pi}{b}\right) \\
 E_y &= B \frac{\gamma_{mn}}{k_c^2} \frac{n\pi}{a} \sin\left(\frac{m\pi}{a}x\right) \cos\left(\frac{n\pi}{b}\right) \\
 E_z &= A \sin\left(\frac{m\pi}{a}x\right) \sin\left(\frac{n\pi}{b}\right) \\
 H_x &= -\frac{1}{Z_{TM}} H_y \\
 H_y &= \frac{1}{Z_{TM}} H_x \\
 H_z &= 0
 \end{aligned} \tag{2}$$

The constant  $B$  is related to the power of the wave [12]. The parameters  $\gamma_{mn}$ ,  $k_c$ , parameters are listed in Table 1. The constants  $A$  and  $B$  in equations affect the amplitude of the fields, but do not affect the field distribution. The field distributions of several typical TE and TM modes are shown in [12].

### 2.3. Principle of Network Analyzers

Network analyzers are widely used to measure the four elements in a scattering matrix:  $S_{11}$ ,  $S_{12}$ ,  $S_{21}$ , and  $S_{22}$ . As shown in Figure 2(a), a network analyzer mainly consists of a source, signal separation devices, and detectors. Basically, a network analyzer can measure the four waves independently: two forward traveling waves  $a_1$  and  $a_2$ , and two reverse traveling waves  $b_1$  and  $b_2$  [12].

As shown in Figure 2(b), the responses of a network to external circuits can also be described by the input and output microwave waves [12]. The input waves at port 1 and port 2 are denoted as  $a_1$  and  $a_2$ , respectively, and the output waves from port 1 and port 2 are denoted as  $b_1$  and  $b_2$ , respectively. These parameters ( $a_1$ ,  $a_2$ ,  $b_1$ , and  $b_2$ ) may be voltage or current, and in most cases, we do not distinguish whether they are voltage or current [12]. The relationships between the input wave  $[a]$  and output wave  $[b]$  are often described by scattering parameters  $[S]$ :

$$[b] = [S][a]; \quad [S] = \begin{bmatrix} S_{11} & S_{12} \\ S_{21} & S_{22} \end{bmatrix}$$

$$S_{jj} = \frac{b_j}{a_j} \quad (j = 1, 2) \quad (3)$$

$$S_{ij} = \frac{b_i}{a_i} \quad (i \neq j; i = 1, 2; j = 1, 2)$$

The reflection coefficient [12];

$$\Gamma_j = S_{jj} = \frac{b_j}{a_j} \quad (4)$$

The transmission coefficient [12];

$$T_{j \rightarrow i} = S_{ii} = \frac{b_i}{a_i} \quad (5)$$

The scattering parameters can then be obtained by the combinations of these four waves according to Eqs.  $S_{ii}$  and  $S_{ij}$ . The four detectors, labeled by  $a_1$ ,  $a_2$ ,  $b_1$ , and  $b_2$  are used to measure the four corresponding waves respectively, and the signal separation devices ensure the four waves to be measured independently [12].

Nicolson and Ross [14] and Weir [15] combined  $S_{11}$  and  $S_{21}$  and derived explicit formulas for the calculation of permittivity and permeability. The algorithm is usually called Nicolson-Ross-Weir (NRW) algorithm [12].

In the NRW algorithm, the reflection and transmission are expressed by the scattering parameters  $S_{11}$  and  $S_{21}$ . The reflection coefficient is given by [12];

$$\Gamma = K \pm \sqrt{K^2 - 1} \quad (6)$$

with

$$K = \frac{(S_{11}^2 - S_{21}^2) + 1}{2S_{11}} \quad (7)$$

The transmission coefficient [12];

$$T = \frac{(S_{11} + S_{21}) - \Gamma}{1 - (S_{11} + S_{21})\Gamma} \quad (8)$$

### 3. EXPERIMENTAL

#### 3.1. Preparation of Nano-particles $\text{Co}_x\text{Mn}_{1-x}\text{Fe}_2\text{O}_4$

Nanoparticles of  $\text{Co}_x\text{Mn}_{1-x}\text{Fe}_2\text{O}_4$  have been prepared by surfactant-assisted hydrothermal process using CTAB. According to this method, 0.003 mol. surfactant cetyltrimethylammonium (CTAB) was dissolved in 35 ml. deionized water to form a transparent solution. The synthesis processes have been presented in detail by Bayrakdar [13].

#### 3.2. $\text{Co}_x\text{Mn}_{1-x}\text{Fe}_2\text{O}_4$ Nanoparticles and Acrylated Epoxy Composite Process

Powders of  $\text{Co}_x\text{Mn}_{1-x}\text{Fe}_2\text{O}_4$  and Acrylated epoxy are taken in weight ratio of 5 :  $x$  : 1 ( $x$  is not disclosed) in a glass bottle, which were thoroughly mixed, and then silver hexafluoroantimonate was used as initiator for polymerization process in the glass bottle in the oven at 150°C. They were mixed and waited for 2 days for polymerization process. After this polymerization process was finished, this polymer was homogenized in mortar and then poured in the mould with  $a = 19.4$  mm,  $d$  (cross section length) = 21.5 mm and  $c$  (thickness) = 2 mm and waited 20 min. at room temperature [13].

#### 3.3. Measurements

The electromagnetic properties of samples were investigated using Agilent 8364B PNA Vector Network Analyzer.

Particles were measured by Size Malvern Instruments Zeta Sizer Nano-ZS.

Magnetic measurements were carried out with a Quantum Design Vibrating Sample Magnetometer (VSM) Model 6000.

SEM imaging was performed using a Philips XL30 SFEQ.

## 4. RESULTS AND DISCUSSION

### 4.1. Structural Properties

Figure 3 shows SEM micrographs of  $\text{Co}_x\text{Mn}_{1-x}\text{Fe}_2\text{O}_4$  ferrites nanoparticles. Nanoparticles of  $\text{Co}_x\text{Mn}_{1-x}\text{Fe}_2\text{O}_4$  were analyzed by XRD in order to investigate the crystalline phases. XRD results were investigated in [13]. Particles' size of  $\text{Co}_x\text{Mn}_{1-x}\text{Fe}_2\text{O}_4$  NPs was obtained as 62 nm for  $x = 0$ , 60 nm for  $x = 0.5$ , and 58 nm for  $x = 1$  from nanosize measure of Zeta Sizer Nano-ZS instrument results [13, 16].

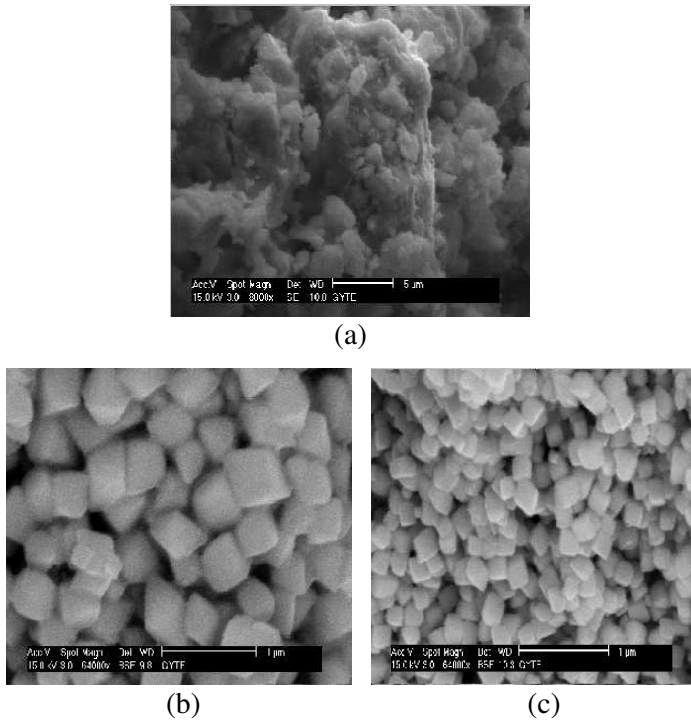


**Figure 3.** SEM images of (a)  $\text{CoFe}_2\text{O}_4$ , (b)  $\text{Co}_{0.5}\text{Mn}_{0.5}\text{Fe}_2\text{O}_4$  and (c)  $\text{MnFe}_2\text{O}_4$  spinel ferrites.

**Table 2.** Saturation magnetization values of  $\text{Co}_x\text{Mn}_{1-x}\text{Fe}_2\text{O}_4$  nanoparticles at room temperature.

$\text{Co}_x\text{Mn}_{1-x}\text{Fe}_2\text{O}_4$	$M_s$ (emu/gr)
$x = 0.0$	31.98
$x = 0.5$	1.46
$x = 1.0$	84.90

#### 4.2. Magnetization Measurements

Magnetization measurements of  $\text{Co}_x\text{Mn}_{1-x}\text{Fe}_2\text{O}_4$  nanoparticles were performed using the VSM technique, and the results of  $M-H$  curves of the sample were showed in Figure 4 at room temperature. Saturation magnetization values ( $M_s$ ) of  $\text{Co}_x\text{Mn}_{1-x}\text{Fe}_2\text{O}_4$  nanoparticles were given in Table 2.

Figure 4 shows the magnetization loops of the  $\text{Co}_x\text{Mn}_{1-x}\text{Fe}_2\text{O}_4$  at

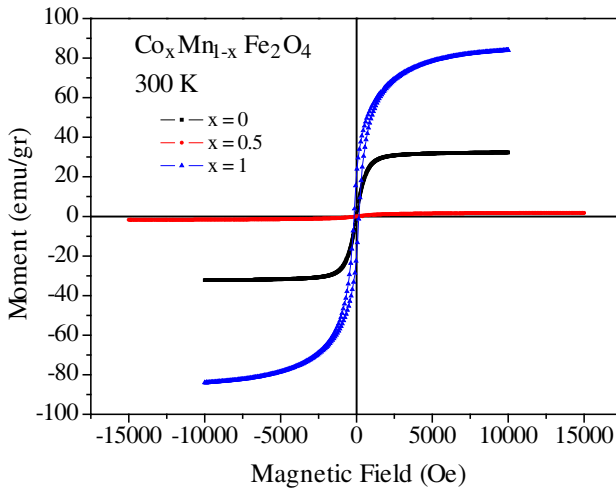


**Figure 4.** The hysteresis loops of this nanocomposite material the room temperature.

room temperature, and magnetic moment values are shown in Table 2. The coercivity ( $H_c$ ) of a magnetic material is generally a measure of its magneto-crystalline anisotropy [17–21].  $\text{CoFe}_2\text{O}_4$  magnetic moment value is higher than other samples. These results show that Co contents attributed to the anisotropic properties of Mn [17–21]. Magnetization measurements of  $\text{Co}_x\text{Mn}_{1-x}\text{Fe}_2\text{O}_4$  samples were performed using the quantum design vibrating sample magnetometer (VSM) technique, and the M-H curves of the sample were investigated at room temperature for all samples. As a result, a typical superparamagnetic ‘S’-like shape of hysteresis curves (without open loops-coercive fields are zero) were observed. These results can be explained as that Co contents attributed to the anisotropic properties of Mn [17–21].

These materials can be used for EMI and absorbing materials [22].

#### 4.3. Microwave Measurements

Measurements were made using rectangular waveguide technique. The experimental setup and theory of absorbing were investigated in [13].

Special manufacture sample holder is shown in Figure 1(b), and this sample holder is very regular. Samples were put into a rectangular-shaped holder of size  $a = 19.4\text{ mm}$ ,  $d$  (cross section length)  $= 21.5\text{ mm}$  and  $c$  (thickness)  $= 2\text{ mm}$  to fit in rectangular waveguides and connected between two waveguides with screws [13]. A special manufacture sample holder is well connected between two

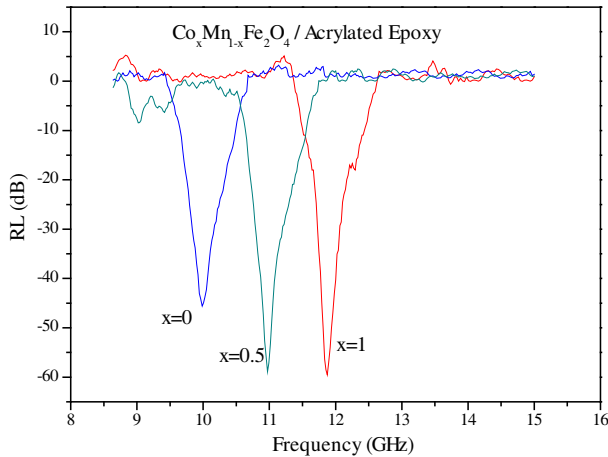


**Figure 5.** Absorption spectra of nanocomposites samples.

**Table 3.** Reflection loss values of  $\text{Co}_x\text{Mn}_{1-x}\text{Fe}_2\text{O}_4/\text{Acrylated epoxy}$  nanocomposites.

$\text{Co}_x\text{Mn}_{1-x}\text{Fe}_2\text{O}_4$	Reflection Loss (dB)
$x = 0.0$	-45.57
$x = 0.5$	-58.08
$x = 1.0$	-59.60

rectangular waveguides with screws, and they are not separated from each other. So, microwave does not come out. Figure 5 shows the measured absorption spectra for prepared polymer-nanoparticles composites. In the present studies, optimized thickness is 2 mm for the sample. This sample shows maximum reflection loss of  $-59.60$  dB and given in Table 3. These can be explained on basis of the impedance matching criterion of a very good absorber [14, 20–34] as follows: In case of a single layered absorber, the normalized input impedance ( $Z$ ) with respect to the impedance in free space and reflection loss (RL) with respect to the normal incident plane wave are given by [7, 12, 13, 16, 17, 22–36]:

$$Z = \sqrt{\mu_r/\varepsilon_r} \tanh \left[ \frac{-i2\pi f d}{c} \sqrt{\mu_r \varepsilon_r} \right] \tag{9}$$

$$RL \text{ (dB)} = -20 \log_{10} \left[ \frac{Z - 1}{Z + 1} \right]$$

where,  $\mu_r$  and  $\varepsilon_r$  are the relative complex permeability and permittivity

of the absorber medium.  $f$  and  $c$  are the frequency of microwave in free space and the velocity of light, respectively.  $d$  is the sample thickness. The reflection loss for sample thickness of 2 mm in the frequency range of 8–20 GHz was made for preparing these composites [7].

## 5. CONCLUSION

Ferrite-polymer nanocomposite structures have been successfully synthesized. The electromagnetic propagation and absorption properties of these nanocomposite materials at 8–20 GHz in microwave guides were theoretically and experimentally investigated. The microwave absorption, magnetization, EMI shielding of  $\text{Co}_x\text{Mn}_{1-x}\text{Fe}_2\text{O}_4/\text{Acrylated Epoxy}$  nanocomposite were analyzed. These microwave absorbers using synthesized prepared composite have been fabricated and successfully demonstrated for a maximum reflection loss of  $-59.60$  dB at 12 GHz with a bandwidth of approximately 2 GHz in a sample with thickness of 2 mm. Our results indicate that the nanocomposite substructures exhibit good absorption performances. The reflection loss is very high, and the bandwidth is higher than that normally reported. It can be said that these samples will provide great benefits for electromagnetic applications and EMI shielding characteristics. In conclusion, the ferrite-polymer ( $\text{Co}_x\text{Mn}_{1-x}\text{Fe}_2\text{O}_4/\text{Acrylated Epoxy}$ ) nanocomposites exhibited good EM absorption properties. The nanocomposites showed higher EM absorption frequency and wider absorption bandwidth ( $\text{RL} < -20$  dB) due to the larger magnetic anisotropy of Co ferrite nanoparticles. Our work suggests that ferrite-polymer ( $\text{Co}_x\text{Mn}_{1-x}\text{Fe}_2\text{O}_4/\text{Acrylated Epoxy}$ ) nanocomposites can be used as a good EM absorption material in 8–20 GHz range.

## REFERENCES

1. Wickenden, B. V. A. and W. G. Howell, "Ferrite quarter wave type absorber," *1st Conf. Roc. Military Microwaves*, 310–317, 1978.
2. Abbas, S. M., A. K. Dixit, R. Chatterjee, and T. C. Goel, "Complex permittivity, complex permeability and microwave absorption properties of ferrite-polymer composite," *J. Magn. Mater.*, Vol. 309, 20–24, 2007.
3. Maeda, T., S. Sugimoto, T. Kagotani, N. Tezuka, and K. Inomata, "Effect of the soft/hard exchange interaction on natural resonance frequency and electromagnetic wave absorption of the rare earth-iron-boron compounds original research article," *J. Magn. Mater.*, Vol. 281, 195–205, Oct. 2004.

4. Jing, L., G. Wang, Y. Duan, and Y. Jiang, "Synthesis and electromagnetic characteristics of the flake-shaped barium titanate powder," *J. of All. and Com.*, Vol. 475, 862, 2009.
5. Lim, K. M., M. C. Kim, K. A. Lee, and C. G. Park, "Electromagnetic wave absorption properties of amorphous alloy ferrite epoxy composites in quasi microwave band," *IEEE Trans. Mag.*, Vol. 39, 1836, 2003.
6. Sugimoto, S., K. Okayama, and S. Kondo, "Barium M-type ferrite as an electromagnetic microwave absorber in the GHz range," *Mater. Trans.*, Vol. 39, 1080, 1998.
7. Lakshmi, K., H. John, K. T. Mathew, R. Joseph, and K. E. George, "Microwave absorption reflection and EMI shielding of PU-PANI composite," *Acta Materialia*, Vol. 57, 371, 2009.
8. Zabetakis, D., M. Dinderman, and P. Schoen, "Metal-coated cellulose fibers for use in composites applicable to microwave technology," *Adv. Mater.*, Vol. 17, 734, 2005.
9. Da Silva, J. B. and N. D. S. Mohallem, "Preparation of composites of nickel ferrites dispersed in silica matrix," *J. Magn. Magn. Mater.*, Vol. 226, 230, 2001.
10. Arshak, K. I., A. Ajina, and D. Egan, "Development of screen-printed polymer thick film planar transformer using Mn-Zn ferrite as core material," *Microelectron J.*, Vol. 32, 113, 2001.
11. Hwang, Y., "Microwave absorbing properties of Ni-Zn ferrite synthesized from waste iron oxide catalyst," *Materials Letters*, Vol. 60, 3277, 2006.
12. Chen, L. F., C. K. Ong, and C. P. Neo, *Microwave Electronics Measurement and Materials Characterization*, John Wiley & Sons, Ltd., 2004,
13. Bayrakdar, H., "Complex permittivity, complex permeability and microwave absorption properties of ferrite-paraffin polymer composites," *J. Magn. Magn. Mater.*, Vol. 323, 1882–1885, 2011.
14. Nicolson, A. M. and G. F. Ross, "Measurement of the intrinsic properties of materials by time-domain techniques," *IEEE Trans. Instrum. Meas.*, Vol. IM-19, 377–382, Nov. 1970.
15. Weir, W. B., "Automatic measurement of complex dielectric constant and permeability at microwave frequencies," *Proc. IEEE*, Vol. 62, 33–36, Jan. 1974.
16. Bayrakdar, H. and K. Esmer, "Dielectric characterization of  $\text{Ni}_x\text{Co}_{1-x}\text{Fe}_2\text{O}_4$  nanocrystals thin film over a broad frequency range (1 MHz – 3 GHz)," *J. Appl. Phys.*, Vol. 107, 044102, 2010.
17. Baykal, A., N. Kasapoglu, Z. Durmuş, H. Kavas, M. S. Toprak,

- and Y. Koseoglu, "CTAB-assisted hydrothermal synthesis and magnetic characterization of  $\text{Ni}_x\text{Co}_{1-x}\text{Fe}_2\text{O}_4$  Nanoparticles ( $x = 0.0, 0.6, 1.0$ )," *Turk. Jour. of Chem.*, Vol. 33, 33, 2009.
18. El Sayed, A. M., "Influence of zinc content on some properties of Ni-Zn ferrites," *Ceram. Int.*, Vol. 28, 363–367, 2002.
  19. Joy, P. A. and S. K. Date, "Effect of sample shape on the zero field cooled magnetization behavior: Comparative studies on  $\text{NiFe}_2\text{O}_4$ ,  $\text{CoFe}_2\text{O}_4$  and  $\text{SrFe}_{12}\text{O}_{19}$ ," *J. Magn. Magn. Mater.*, Vol. 222, 33, 2000.
  20. Huang, X. and Z. Chen, "Nickel ferrite on silica nanocomposites prepared by the sol-gel method," *J. Magn. Magn. Mater.*, Vol. 280, No. 37, 2004.
  21. Kasapoğlu, N., A. Baykal, Y. Köseoğlu, and M. S. Toprak, "Microwave-assisted combustion synthesis of  $\text{CoFe}_2\text{O}_4$  with urea, and its magnetic characterization," *Scripta Materialia*, Vol. 57, 441–444, 2007.
  22. Lee, S. P., Y. J. Chen, C. M. Ho, C. P. Chang, and Y. S. Hong, "A study on synthesis and characterization of the core-shell materials of  $\text{Mn}_{1-x}\text{Zn}_x\text{Fe}_2\text{O}_4$ -polyaniline," *Mat. Sci and Eng. B*, Vol. 143, 2007.
  23. Natio, Y. and K. Suetake, "Application of ferrite to electromagnetic-wave-absorber and its characteristics," *IEEE Trans. Microwave Theory Tech.*, Vol. 19, No. 1, 65, 1971.
  24. Murthy, V. R. and R. Raman, "A method for the evaluation of microwave dielectric and magnetic parameters using rectangular cavity perturbation technique," *Solid State Commun.*, Vol. 70, No. 8, 847, 1989.
  25. Verma, A., A. K. Saxena, and D. C. Dube, "Microwave permittivity and permeability of ferrite-polymer thick films," *J. Magn. Magn. Mater.*, Vol. 263, Nos. 1–2, 228, 2003.
  26. Arit, G., D. Hennings, and G. de With, "Dielectric properties of fine-grained barium titanate ceramics," *J. Appl. Phys.*, Vol. 58, No. 4, 1619, 1985.
  27. Ding, L., X. Wang, and R. V. Gregory, "Thermal properties of chemically synthesized polyaniline (EB) powder," *Synthetic Met.*, Vol. 104, 73, 1999.
  28. Abbas, S. M., M. Chandra, A. Verma, R. Chatterjee, and T. C. Goel, "Complex permittivity and microwave absorption properties of a composite dielectric absorber," *Composites Part A*, Vol. 37, 2148, 2006.
  29. Wu, K. H., T. H. Ting, C. I. Liu, and C. C. Yang,

- “Electromagnetic and microwave absorbing properties of  $\text{Ni}_{0.5}\text{Zn}_{0.5}\text{Fe}_2\text{O}_4$ /bamboo charcoal core-shell nanocomposites,” *Composites Science and Technology*, Vol. 68, 132, 2008.
30. Singh, D., A. Kumar, S. Meena, and V. Agrawala, “Analysis of frequency selective surfaces for radar absorbing materials,” *Progress In Electromagnetics Research B*, Vol. 38, 297–314, 2012.
  31. Sharma, R. and R. C. Agarwala, “Development of radar absorbing nano crystals by microwave irradiation,” *Materials Letters*, Vol. 62, 2233, 2008.
  32. Zhao, D. L., J. M. Zang, and Z. M. Shen, “Electromagnetic and microwave absorbing properties of Co-filled carbon nanotubes,” *Journal of Alloys and Compounds*, Vol. 505, 712, 2010.
  33. Naito, Y. and K. Suetake, “Application of ferrite to electromagnetic wave absorber and its characteristic,” *IEEE Trans. on Micro. Theo. and Tsc.*, Vol. 19, 65–72, 1971.
  34. Kim, S. S., S. B. Jo, K. I. Gueon, K. K. Choi, J. M. Kim, and K. S. Chum, “Complex permeability and permittivity and microwave absorption of ferrite-rubber composite in X-band frequencies,” *IEEE Trans. Mag.*, Vol. 27, 5462–5464, 1991.
  35. Lim, K. M., M. C. Kim, K. A. Lee, and C. G. Park, “Electromagnetic wave absorption properties of amorphous alloy-ferrite-epoxy composites in quasi-microwave band,” *IEEE Trans. Mag.*, Vol. 39, 1836–1841, 2003.
  36. Pinho, M. S., M. L. Gregori, R. C. R. Nunes, and B. G. Soares, “Performance of radar absorbing materials by waveguide measurements for X-and Ku-band frequencies,” *European Polymer Journal*, Vol. 38, 2321–2327, 2002.